Characterization of the Subunit Structure of the Catalytically Active Type I Iodothyronine Deiodinase*

Jack L. Leonard‡, Theo J. Visser§, and Deborah M. Leonard

From the Department of Cellular and Molecular Physiology, University of Massachusetts Medical School, Worcester, Massachusetts 01655 and §Internal Medicine III, Erasmus University Medical School, 3015GD Rotterdam, The Netherlands

Type I iodothyronine deiodinase is a ~50-kDa, integral membrane protein that catalyzes the outer ring deiodination of thyroxine. Despite the identification and cloning of a 27-kDa selenoprotein with the catalytic properties of the type I enzyme, the composition and the physical nature of the active deiodinase are unknown. In this report, we use a molecular approach to determine holoenzyme composition, the role of the membrane anchor on enzyme assembly, and the contribution of individual 27-kDa subunits to catalysis. Overexpression of an immunologically unique rat 27-kDa protein in LLC-PK1 cells that contain abundant catalytically active 27-kDa selenoprotein decreased deiodination by ~50%, and >95% of the LLC-PK1 derived 27-kDa selenoprotein was specifically immune precipitated by the anti-rat enzyme antibody. The hybrid enzyme had a molecular mass of 54 kDa and an $s_{20,w}$ of ~3.5 S indicating that every native 27-kDa selenoprotein partnered with an inert rat 27-kDa subunit in a homodimer. Enzyme assembly did not depend on the presence of the N-terminal membrane anchor of the 27-kDa subunit. Direct visualization of the deiodinase dimer showed that the holoenzyme was sorted to the basolateral plasma membrane of the renal epithelial cell.

Type I thyroxine deiodinase (D1,[1] EC 3.8.1.4) is the most abundant member of a family of membrane-bound enzymes that catalyze the removal of a single iodine atom from thyroid hormone. D1 generates most of the bioactive T_3 found in blood (1–4) and serves as the essential first step in the molecular mechanism of thyroid hormone action *in vivo*.

D1 is a selenoenzyme encoded by an ~2.1-kilobase pair mRNA and is most abundant in liver, kidney, and thyroid (1–5). The ~27-kDa enzyme polypeptide (p27) contains the novel amino acid, selenocysteine (SeC) (5), and this residue is essential for full catalytic activity (6–8). Whether p27 is cata-lytically active itself or requires post-translational modification and/or assembly into a multimeric complex remains to be established. Despite uncertainty about its composition and the physical nature of the catalytically active enzyme, site-directed mutagenesis, species comparisons, domain substitution, and limited deletion analysis (9–14) have been used to characterize some of the functional domains of p27. The p27 polypeptide contains an uncleaved N-terminal signal/membrane anchor followed by an uninterrupted catalytic domain facing the cell interior (10). Iodothyronine substrate specificity is determined by amino acids located between residues 40 and 65, as judged by site-directed mutagenesis, analysis of species-specific differences in catalytic properties, and amino acid composition, and by interspecies deletion-substitution analysis (9, 11). In addition to the presumed membrane anchor and the substrate specificity domain, the active center is thought to be located in an ~15 amino acid long region bracketing the SeC residue (7, 12).

Four D1 amino acid residues (Phe-65, Cys-124, SeC-126, and His-174) have been identified as essential for substrate specificity and catalysis (7, 9, 11, 12–14). The roles of Phe-65 in iodothyronine specificity and of SeC126 in catalysis are well established (7, 9, 11), whereas the roles of Cys-124 and His-174 in the catalytic reaction are less understood. For example, replacement of Cys-124 with alanine led to parallel ~2-fold decreases in the K_m for rT_3 and in catalytic efficiency when assayed at a fixed cofactor concentration (15). Determination of the limiting Michaelis constants using two substrate reaction kinetics revealed that the K_m for rT_3 was marginally affected in the C124A mutant (14, 15), whereas the velocity of the forward reaction decreased ~2-fold (14, 15), and the thiol cofactor requirement increased by 6–14-fold (14, 15). The mechanism for these changes in kinetic parameters is unclear. Traditional chemical modification studies established that histidine(s) were essential for catalysis (16, 17), and subsequent mutagenesis and transient expression studies identified His-174 as one of these essential residue(s) (13).

However, caution is essential when attempting to assign functional significance to individual amino acids in an incompletely characterized enzyme. Whereas the direct participation of any D1 residue that affects catalysis is the first possibility often considered, it is equally likely that individual amino acid substitutions can influence D1 activity by indirect means such as (i) abnormal post-translational processing; (ii) altered folding of the primary translation product that leads to rapid degradation; (iii) improper sorting of the mutant p27 in the Golgi apparatus; and/or (iv) disturbed assembly of a functional enzyme. Thus, the interpretation of the mechanistic consequences of individual mutations on D1 activity in whole cell lysates of transiently transfected cells is difficult at best and cannot identify what molecular events are affected without an

---

[1] The abbreviations used are: D1, type I iodothyronine 5′-deiodinase; T_4, thyroxine; T_3, 3,3′,5′-triiodothyronine; rT_3, reverse T_3; tDOC, taurodeoxycholate; p27, 27-kDa substrate-binding subunit of type I iodothyronine 5′-deiodinase; M4, Ser-126 mutant of rat p27; M4^{GFP}, green fluorescent protein-tagged M4; BrAcT$_4$, *N*-bromoacetyl-L-thyroxine; PAGE, polyacrylamide gel electrophoresis; BSA, bovine serum albumin; SeC, selenocysteine; TEMED, *N,N,N′,N′*-tetramethylethylenediamine; PBS, phosphate-buffered saline.

understanding of the influence of the mutation on enzyme assembly and processing.

Much of the biochemistry of D1 was established prior to the cloning of the enzyme using the alkylating substrate analogs, N-BrAcT$_4$ and N-BrAcT$_3$ (18–21). Affinity labeling studies done with liver and kidney membrane preparations identified an ~27-kDa thyroid hormone-binding protein (p27) (19–21) that was subsequently cloned by functional expression (5). Interestingly, molecular sieve chromatography of the detergent-soluble rat kidney D1 yielded an ~50-kDa functional enzyme (22), and subsequent work showed that the affinity labeled p27 co-migrated with catalytic activity as an ~54-kDa complex (23). These data suggested that the catalytically active D1 was composed of two similarly sized subunits. Whether the functional enzyme is a homodimer of p27 subunits or a heterodimer formed between p27 and an unknown subunit remains to be established. The latter possibility cannot be excluded because kidney-derived cell lines have been used for most, if not all, p27 transient expression studies, and this organ has abundant D1 activity. Thus, it is possible that a 25–30-kDa membrane anchor protein found in kidney cells could partner with p27 to form a functional enzyme.

In this study, we exploited the species differences in the composition of the C terminus of p27 to characterize the composition of catalytically active D1. By using the native D1 found in a pig renal epithelial cell line (LLC-PK1), we overexpressed an immunologically unique, catalytically inert S126 mutant of rat p27 (M4), and we examined the consequences of M4 expression on D1 subunit assembly, enzyme activity, and subcellular trafficking. The data show that catalytically active D1 is a dimer composed of two p27 subunits and that the assembled enzyme is sorted to the basolateral plasma membrane of renal epithelial cells.

EXPERIMENTAL PROCEDURES

Materials—All reagents were of the highest purity commercially available. Restriction endonucleases and DNA-modifying enzymes were purchased from New England Biolabs (Beverly, MA). The femtomoles of DNA sequencing and the Altered Sites Mutagenesis kits were obtained from Promega (Madison, WI). α-^{35}S-dATP (3000 Ci/mmol) and [α-^{32}P]dCTP (800 Ci/mmol) were purchased from PerkinElmer Life Sciences. ^{75}SeO$_3^{2-}$ (~200 Ci/mmol) was purchased from the University of Missouri-Columbia Research Reactor Facility (Columbia, MO). L-(3′- or 5′-^{125}I)rT$_3$ was prepared by radioiodination of 3,3′-T$_2$ using methods described previously (24). The 2.1-kilobase pair p27 cDNA (G21; GenBank™ accession number X57999) was the gift of P. R. Larsen, Harvard Medical School. Synthetic oligonucleotides were prepared in house or purchased from Life Technologies, Inc. All iodothyronines were of the L-configuration and were purchased from Henning Berlin GmbH. Dulbecco's modified Eagle's medium, antibiotics, Hanks' buffered salt solution, glucose, trypsin, and G418 were obtained from Life Technologies, Inc.; supplemented bovine calf serum was from HyClone Laboratories (Boulder, CO); acrylamide and *N,N′*-methylenebisacrylamide were from U. S. Biochemical Corp.; ammonium persulfate and TEMED were from Bio-Rad; and dithiothreitol was from Calbiochem.

Cell Culture—LLC-PK1 cells were grown in 25-cm^2 flasks in a humidified atmosphere of 5% CO_2 and 95% air at 37 °C as described previously (23). Complete Growth Medium was composed of Dulbecco's modified Eagle's medium containing 15 mM sodium bicarbonate, 15 mM HEPES (pH 7.2), 25 mM glucose, 1 mM sodium pyruvate, 5% (v/v) calf serum, 50 milliunits/ml penicillin, and 90 μg/ml streptomycin. Cells were subcultured every 3–5 days by seeding 5×10^4 cells/cm^2 into 25-cm^2 flasks. Culture medium was changed 3 times weekly.

Mutagenesis—Site-directed mutagenesis was used to inactivate the catalytic activity of rat p27 by substituting Ser for the active center SeC. In brief, the 2.1-kilobase pair G21 cDNA was released from pBSK using *Kpn*I-*Xho*I and cloned into the mutagenesis shuttle vector, pALTER-1 (Promega, Madison, WI). A 24-mer synthetic oligonucleotide bracketing the SeC-126 codon (nucleotides 372–396, 5′-CAGCTGCAC-

C̲AGCCCTTCATTTCTT-3′) was used to create an SeC-126 → Ser substitution (underlined nucleotides) using oligonucleotide-based mutagenesis according to the manufacturer's instructions. The integrity of the catalytically inactivated, non-SeC containing the M4 mutant of rat p27 was confirmed by DNA cycle sequencing of the entire coding region (nucleotides 7–780), and M4 was subcloned into the *Kpn*I-*Xho*I site of the eukaryotic expression vector, pcDNA3. Construct orientation was confirmed by analytical restriction digestion.

Elimination of the putative extracellular domain and the membrane-spanning anchor of p27 was done by polymerase chain reaction-based deletion. All upstream oligonucleotide primers contained a *Kpn*I site for subcloning and an in-frame Kozak consensus translation initiation site to ensure adequate expression in mammalian cells. The first 19 amino acids of p27 that include the putative extracellular domain and 7 residues of the membrane-spanning region were deleted using a 27-mer oligonucleotide upstream primer (5′-GGGTACCATGGC̲C̲TTGGAGGT-GGCTAC-3′, nucleotides 65–80 of G21 underlined). The N-terminal 42 amino acids that contain the entire membrane-spanning domain was deleted using a 29-mer oligonucleotide upstream primer (5′-GGGG-TACCATGGCCATGGGCCAAAAGACC-3′, nucleotides 131–150 of G21 underlined). The common downstream primer was a 20-mer oligonucleotide corresponding to nucleotides 895–914 of G21 (5′-GCCTC-CCGGGTAGTTATTTG-3′). Polymerase chain reaction was done using Vent® DNA polymerase (Stratagene, La Jolla CA) for a total of 25 cycles according to the following temperature profile: 95 °C, 1.0 min; 50 °C, 1.0 min; 72 °C, 3.0 min, with a final 10-min extended incubation at 72 °C. Polymerase chain reaction products were digested with *Kpn*I to generate asymmetric ends for subcloning, and gel was isolated on 1.4% low melt agarose gels and ligated into the *Kpn*I-*Sma*I-ended pcDNA3-M4. The N-terminal 19-residue deletion mutant, M4-19, and the N-terminal 42-residue deletion mutant, M4-42, were confirmed by DNA cycle sequencing (see below).

Generation of M4-expressing LLC-PK1 Cells—LLC-PK1 cells were grown in Growth Medium to 60% confluence and transfected with 10 μg of pcDNA3 (empty vector control) or 10 μg of pcDNA3-M4, pcDNA3-M4-19, or pcDNA3-M4-42 using cationic liposomes (DOTAP®, Roche Molecular Biochemicals) according to the manufacturer's instructions. Stable transfectants were selected with 800 μg/ml G418, and antibiotic-resistant cells were expanded without clonal isolation. Cells constitutively expressing M4 (S126 cells), M4-19, and M4-42 were maintained in 200 μg/ml G418 to prevent loss of expression of the exogenous gene product.

DNA Sequencing—Double-stranded DNA sequencing was done by the dideoxynucleotide method of Sanger (see Ref. 25) using cycle sequencing and iterative primers. All sequence information was confirmed by sequencing both strands.

Biosynthetic Labeling of Native p27^{wt} Selenoprotein in S126 Cells—S126 cells were grown to 90% confluence in 25-cm^2 flasks in Complete Growth medium. Cell monolayers were washed 3 times with serum-free Dulbecco's modified Eagle's medium, and the medium was replaced with serum-free ^{75}Se labeling medium composed of Dulbecco's modified Eagle's medium supplemented with 25 mM HEPES (pH 7.2), 10 mg/ml BSA, 10 μg/ml transferrin, 20 μg/ml insulin, 40 nM ^{75}Se (specific radioactivity, 200 μCi/nmol), and antibiotics. Cellular selenoproteins were biosynthetically radiolabeled at 37 °C for 48 h. After labeling, cells were washed free of labeling medium, scraped from the dish, and collected by centrifugation. Cell pellets were stored at −70 °C until use.

Production of Species-specific, Anti-p27 Antibodies—Comparison of the p27 from fish to man revealed that the C terminus of p27 shows species-specific variations, and the rodent p27 contains a C-terminal extension of 8–12 amino acids (26). This unique feature was exploited to generate a rodent-specific, anti-p27 antibody. A synthetic peptide corresponding to the C-terminal 21 residues of rat p27 (NH$_2$-YEEVRAV-LEKLCIPPGHMPQF-COOH) was coupled to mollusk hemocyanin and used to immunize rabbits. An N-terminal tyrosine was included to allow radioiodination and to facilitate directional coupling of the p27 peptide to carrier protein by diaminobenzidine condensation. Where indicated, rodent-specific anti-p27 IgG was purified by affinity chromatography using a p27 peptide-Affi-Gel affinity matrix. In brief, primary antiserum was adsorbed to the p27 peptide-Affi-Gel 10 matrix at 25 °C, and unbound proteins were removed by repeated washes with 150 mM NaCl, 20 mM sodium phosphate buffer (pH 7.4). Anti-p27 IgG was eluted with 100 mM Hac, and antibody elution was monitored by absorbance at 280 nm. Fractions containing antibody were neutralized by adding 0.1 volume of 1 M Tris (pH 8.6), pooled, and stored frozen (−70 °C) at ~1 mg/ml IgG until use.

Antibody Characterization—Anti-p27 antibodies were used for immunoprecipitation and in a competitive binding assay. Pull-down as-

---

[2] J. L. Leonard, T. J. Visser, and D. M. Leonard, manuscript in preparation.

says of M4 and associated proteins were done for 60 min at 4 °C in a total volume of 100 μl. Precipitation reactions contained 50–100 units of tDOC-solubilized D1 activity prepared from purified membranes (23), 100 mM HEPES buffer (pH 8.0), 100 mM NaCl, 0.1 mM PMSF, 5 mM tDOC, 10 μl of immobilized rProtein A™ beads (RepliGen, Cambridge, MA), and either preimmune rabbit antisera or anti-rat p27 antisera (1:100 final dilution). Where indicated, excess C-terminal p27 peptide (10 μg/ml, final concentration) was added to block antibody-binding sites. Immune complexes bound to the protein A beads were removed by centrifugation, and the deiodinase activity remaining in the clarified supernatant was determined as described below.

M4 expression in LLC-PK1 cells was quantified by a competitive binding assay. Cell pellets or isolated membrane preparations were solubilized with either 0.1% Triton X-100 (v/v) or 5 mM tDOC, and the soluble enzyme preparation was clarified by centrifugation at 14,000 × g for 30 min at 4 °C. Assays were done in triplicate in a total of 100 μl containing 100 mM Tris buffer (pH 8.3), 100 mM NaCl, 5 mM tDOC, 10,000 cpm ^{125}I-labeled p27 peptide (specific radioactivity, 100 mCi/μmol), anti-p27 antisera (1:50,000 final dilution), and detergent extracts. Incubations were done for 2 h at 4 °C, and immune complexes were precipitated by addition of goat anti-rabbit antiserum (1:5000 dilution). After an additional 60 min at 4 °C, 400 μl of ice-cold PBS containing 10 mg/ml BSA was added, and the immune precipitates were collected by centrifugation. Pellets were counted in a well-type γ-counter. Shown in Fig. 1*A* is a representative displacement curve comparing p27 peptide to detergent extracts containing the rodent p27 (rat kidney) to that pig p27 (LLC-PK1 cells). The minimum detection limit of rodent p27 is ~3 fmol per assay tube (81 pg of p27/tube), and the maximum binding capacity of the rabbit anti-rat p27 antisera is 22 nmol of p27/ml antisera as determined by Scatchard analysis of the binding data.

Construction of GFP-tagged M4 Expression Plasmids—A green fluorescent protein (GFP)-tagged p27 fusion construct (M4^{GFP}) was generated by appending GFP to the C terminus of M4. In brief, the ~750-base pair *Hin*dIII fragment (containing the M4 mutant of p27-coding sequence lacking the C-terminal 11 amino acids) was excised from pcDNA3-M4, gel-purified, and ligated, in-frame, into the *Hin*dIII site of pEGFP-N1 (CLONTECH, Palo Alto, CA). The fusion construct M4^{GFP} cDNA was excised with *Bam*HI and *Not*I and ligated into *Bam*HI-*Not*I-ended pcDNA3. The integrity of the fusion construct and expression of a fluorescent fusion protein were confirmed by transient expression of the pcDNA3-M4^{GFP} in HEK293 cells and immunoblot analysis using anti-GFP IgG (CLONTECH, CA).

Photomicroscopy—Cells were seeded onto poly-D-lysine (10 μg/ml)-coated glass coverslips (22 × 22 mm) and grown to ~60% confluence. Cells were then fixed with 4% paraformaldehyde and permeabilized with 0.1% Triton (v/v) in PBS. Similarly, rat kidney slices were fixed with 4% paraformaldehyde in PBS, embedded in paraffin, and ~4-μm sections were prepared from the outer cortex. The distribution of p27 in the renal tubule was determined using affinity-purified, anti-p27 IgG (0.1 μg/ml). Immune complexes were visualized using a Texas Red-conjugated goat, anti-rabbit IgG (1:2, 500 final dilution). The distribution of M4^{GFP} in LLC-PK1 cells was determined by fluorescence microscopy. Digital images were captured using a Spot CCD camera (Meyer Instruments, Inc, Houston, TX) and processed using Adobe Photoshop software. Photomicrographs shown are representative of 20–30 independent fields.

Analytical Procedures—D1 activity was determined in cell lysates by measuring the release of radioiodide from 10 μM [^{125}I]rT$_3$ (100 cpm/pmol) at 20 mM dithiothreitol (unless otherwise indicated) in a total volume of 100 μl. Deiodination reactions were done, in triplicate, in 100 mM potassium phosphate buffer (pH 7.0), 1 mM EDTA, with 10–25 μg of cell protein and incubated at 37 °C for 10–20 min. Product formation was measured as described previously (24), and the data are expressed as units/mg protein where 1 unit equals 1 pmol of I⁻ released per min.

All experiments were performed at least three times. Statistical analysis was done by Student's *t* test.

RESULTS

Characterization of the Rodent-specific Anti-p27 Antisera—The characterization of the anti-rat p27 antibody was done using a competitive binding assay, immunoprecipitation, and immunocytochemistry as shown in Fig. 1. Detergent-soluble rat kidney p27 readily displaced ^{125}I-labeled p27 peptide from the anti-rat p27 antisera (Fig. 1*A*) yielding a concentration of p27 of 4 ± 1 pmol of p27 per mg of kidney membrane protein (mean ± S.E., *n* = 3), similar to that reported previously (19,
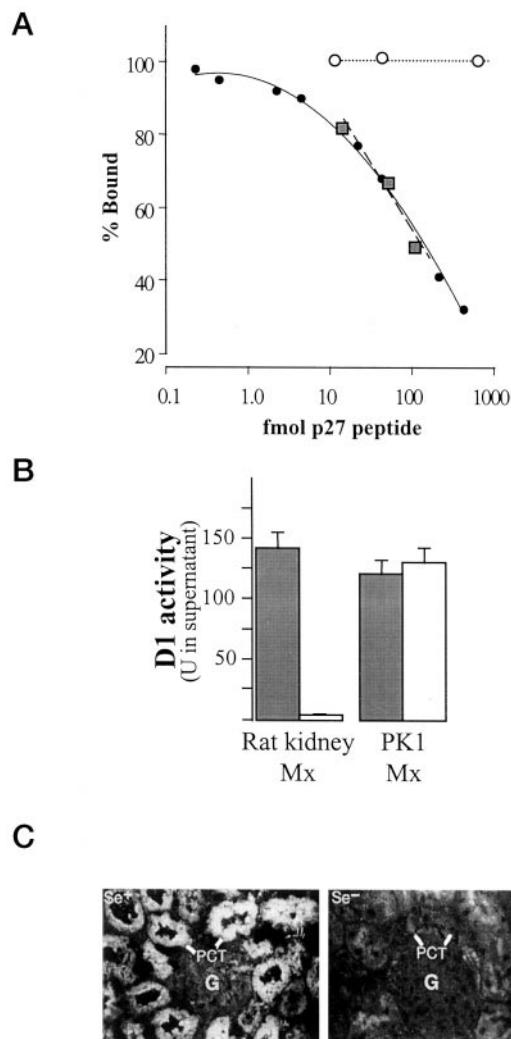

Fig. 1. **Characterization of the epitope-directed anti-rat p27 antisera.** *A,* competitive binding analysis of p27 peptide, detergent-soluble rat kidney membranes, and detergent-soluble LLC-PK1 cell membranes. Cell and membrane preparations were solubilized with 0.1% Triton X-100 or 5 mM tDOC. Assays were done as described under "Experimental Procedures." Data are reported as the means of closely agreeing triplicate determinations. ●, p27 peptide; ■, rat Mx; ○, LLC-PK1 Mx. *B,* immune precipitation of D1 activity from solubilized rat kidney membranes (*rat Mx*) and solubilized LLC-PK1 (*PK1 Mx*) membranes. Microsomes were prepared from rat kidney and LLC-PK1 cells. Catalytically active D1 was solubilized with 5 mM tDOC, and 2 mg of soluble Mx protein (150 units of D1 activity) was incubated in triplicate with a 1:100 dilution of anti-rat p27 antisera in the absence (*filled bars*) and presence (*open bars*) of 10 μg/ml blocking peptide at 4 °C for 60 min. D1 activity remaining in the supernatant after removal of specific immune complexes by protein A beads was determined as described under "Experimental Procedures." Data are reported as means ± S.E. of three independent microsome preparations. *C,* representative photomicrographs of immunoreactive p27 in rat kidney tubules from selenium-supplemented and selenium-deficient rats. *PCT*, proximal convoluted tubule; *G,* glomerulus. *Bar* = 50 μm.

20). On the other hand, up to 1 mg of LLC-PK1 membrane protein (~500 units of D1 activity) failed to displace any of the rat-specific ^{125}I-labeled p27 peptide indicating that the pig p27 selenoprotein was not recognized by the anti-rat p27 antibody. The ability of the anti-rat p27 antisera to immune precipitate detergent-soluble D1 activity is shown in Fig. 1*B*. Detergent-soluble D1 activity was prepared from rat kidney and LLC-PK1 microsomes (23), and the clarified extracts were incubated with anti-p27 antibody in the absence or presence of excess blocking peptide. All (>98%) of the soluble D1 activity from rat kidney membranes was lost from the detergent extracts when the
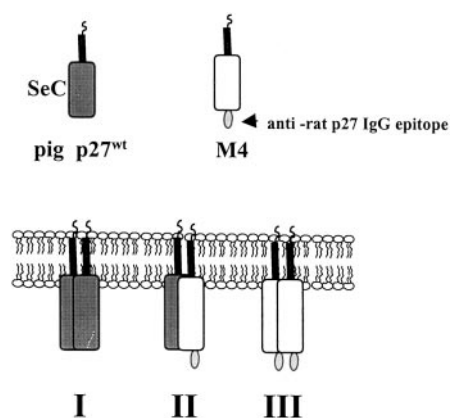
FIG. 2. **Potential combinations of p27 molecules in LLC-PK1 cells constitutively expressing the Ser-126 mutant (M4) of rat p27.**

immune complexes were removed with protein A-Sepharose, and addition of a 200-fold molar excess of p27 peptide completely blocked the antibody-dependent loss of D1 activity. As expected from the failure of the LLC-PK1-derived p27 to displace the rat p27 peptide from the anti-rat p27 antibody, no soluble D1 activity was immune precipitated from microsomes isolated from LLC-PK1 cells. Shown in Fig. 1*C* are representative photomicrographs of rat renal cortex from selenium-replete and selenium-deficient rats stained with the anti-rat p27 antisera. Selenium-dependent expression of the abundant immunoreactive protein is found in cells lining a subset of tubules that surround the glomerulus, consistent with earlier subcellular localization studies (23, 27). These data establish that the anti-rat p27 antiserum shows species-specific recognition of the rat p27 selenoprotein by immunoprecipitation, competitive displacement analysis, and by immunocytochemistry.

Analysis of the Effects of Constitutive Expression of M4 on Native D1 Activity in LLC-PK1 Cells—The abundant D1 activity in LLC-PK1 cells was used previously to characterize both the biochemistry and physiochemical properties of the enzyme (23, 28). Gel filtration and isopycnic density gradient centrifugation of detergent-soluble D1 from these cells showed that catalytic activity and the BrAcT$_4$-labeled p27 co-migrated as a globular protein with a M_r of ~54,000 (28), suggesting that D1 is a dimer of two similarly sized subunits, presumably p27. Shown in Fig. 2 are the potential combinations of p27 subunits that can form in LLC-PK1 cells that constitutively express the catalytically inert M4 mutant of rat p27 (S126 cells). Combinations I and II yield dimers with at least one selenoprotein partner. Overexpression of the M4 protein relative to the native p27^{wt} selenoprotein will also generate immunoreactive, nonselenoprotein dimers of M4 (combination III), and these dimers are favored if the rat-derived, M4 mutant cannot interact with the native p27^{wt} in LLC-PK1 cells. Only combination II yields a D1 dimer composed of a native p27^{wt} selenoprotein partnered with M4, and this hybrid D1 can be rescued with antibodies directed against the rat p27.

Shown in Fig. 3 are the results of pull-down assays done with anti-rat p27 antibody and soluble D1 from control (vector) and S126 cells. Little, if any, detergent-soluble ^{75}Se-labeled p27 was specifically bound to the protein A beads when normal rabbit serum was used (Fig. 3*A, left bars*). In contrast, ~10% of the total ^{75}Se-labeled protein(s) solubilized from S126 cells was specifically immune precipitated by the anti-rat p27 antibody, whereas the quantity of ^{75}Se-labeled proteins from the vector cells bound to the protein A beads was identical to the nonspecific binding found when normal rabbit serum was used (Fig. 3*A*). Addition of a 200-fold molar excess of blocking peptide
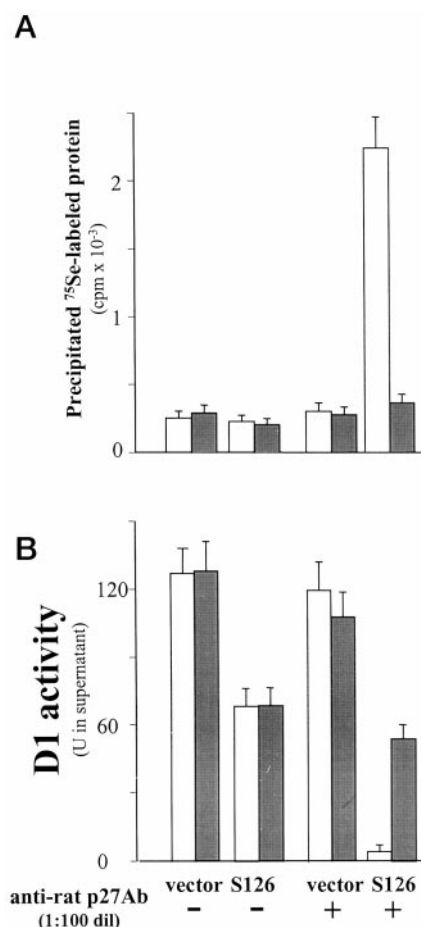

FIG. 3. **Immunoprecipitation of D1 holoenzyme composed of pig p27^{wt}-M4 dimers by anti-rat p27 antisera.** *A,* immune precipitation of ^{75}Se-labeled proteins. LLC-PK1 cells that constitutively express the *neo^r* gene (vector cells) or the M4 mutant of p27 (S126 cells) were grown in ^{75}Se-labeling media for 48 h as described under "Experimental Procedures." Cell membranes were prepared, and 25,000 cpm ^{75}Se-labeled protein was incubated with protein A beads, ± anti-rat p27 IgG in the absence (*open bars*) and presence (*filled bars*) of excess blocking peptide as described in the legend to Fig. 1*B*. *B,* immune precipitation of D1 activity. The ability of anti-rat-p27 antisera to immunoprecipitate tDOC-soluble D1 from vector and S126 cell microsomes was done as described in the legend to Fig. 1*B*. Data are reported as means ± S.E., $n = 3$ independent preparations.

decreased the quantity of ^{75}Se-labeled S126 cell protein bound to the anti-rat p27 antibody to that nonspecifically bound to the protein A beads.

Shown in Fig. 3*B* is the companion analysis of the effects of anti-rat p27 antibody on soluble D1 activity prepared from microsomes isolated from vector and S126 cells. Similar to the results obtained with soluble ^{75}Se-labeled p27 prepared from vector and S126 cells, <5% of the soluble D1 activity was lost in the pull-down assay when normal rabbit serum was used, and the addition of excess blocking peptide had no effect on D1 activity. Interestingly, the D1 activity in S126 cells was ~50% of that found in the vector control, LLC-PK1 cell. Just as observed with the soluble D1 activity from rat kidney and untransfected LLC-PK1 cells (see Fig. 1*B*), little, if any, soluble D1 activity in vector cells was removed by immune precipitation with anti-rat p27 antisera. In contrast, >95% of the D1 activity in detergent extracts of S126 cells was removed by the anti-rat p27 antibody, and this loss in activity was blocked by addition of excess p27 peptide (Fig. 3*B*). By comparing the quantity of soluble D1 remaining in the supernatant in the presence of excess blocking peptide with that found when normal rabbit serum was used revealed that ≥97% of the starting
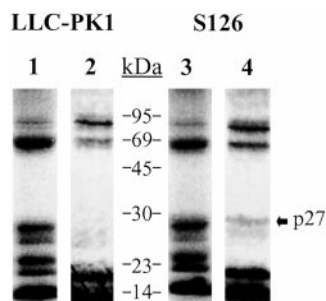
FIG. 4. **Representative fluorograms of SDS-PAGE analysis of anti-rat p27 immune precipitates from control LLC-PK1 cells or M4-expressing S126 cells.** Immune precipitates were prepared as described under "Experimental Procedures," denatured by heating at 100 °C for 5 min, and separated on 12.5% SDS-PAGE cells under reducing conditions as described previously (23). Proteins were resolved by SDS-PAGE, and the distribution of ^{75}Se-labeled proteins was determined by PhosphorImager. *Lane 1,* LLC-PK1 cell lysate; *lane 2,* immune precipitate from LLC-PK1 cells; *lane 3,* S126 cell lysate; *lane 4,* immune precipitate from S126 cells.

D1 activity in the S126 cell was protected from antibody depletion by the blocking peptide. These findings show that overexpression of the catalytically inert M4 protein markedly reduced the catalytic potential of the native D1 in the host LLC-PK1 cell and yielded a "hybrid" D1 that was specifically precipitated by anti-rat p27 antibodies. The data also suggest that the assembly of a catalytically active D1 is a post-translational event.

Direct identification of hybrid D1 dimers composed of the non-selenoprotein M4 and the native p27^{wt} selenoprotein is shown in Fig. 4. The native p27 selenoprotein in control LLC-PK1 cells and in S126 cells was biosynthetically radiolabeled with ^{75}Se, and detergent extracts of the radiolabeled cells incubated with anti-rat p27 antibody and the specific immune complexes were separated on 12.5% SDS-PAGE gels. Shown in Fig. 4 are representative fluorograms of the ^{75}Se-labeled proteins in starting cell lysates (*lanes 1* and *3*) and in immune precipitates (*lanes 2* and *4*) of control LLC-PK1 cells (*lanes 1* and *2*) and S126 cells (*lanes 3* and *4*). Whereas M4 overexpression had little, if any, influence on the quantity of ^{75}Se-labeled p27 found in S126 cell lysates (compare *lanes 1* and *3*), the native ^{75}Se-labeled p27 co-immunoprecipitated with M4 from the S126 cell (*lane 4*) but was not immune precipitated from the parent LLC-PK1 cells (*lane 2*). Since only the native p27 can incorporate ^{75}Se into the polypeptide, these data confirm that the native LLC-PK1-derived p27 subunit was partnered with a rat M4 polypeptide in the S126 cell. Together with the data showing that specific M4-directed antibodies removed >97% of the D1 activity from the S126 cell, these data show that overexpression of the inert M4 leads to the quantitative formation of a catalytically impaired, hybrid D1 enzyme composed of pig p27^{wt}-M4 partners.

We then measured the quantities of both the native p27^{wt} and M4 mutant proteins in the S126 cells by exploiting the selenium-dependent expression of the p27^{wt} and the unique immunoreactivity of M4. S126 cells were grown in the absence and presence of 40 nM ^{75}Se for 48 h, and cell lysates were prepared. Selenium-deficient S126 cells lost >93% of the hybrid D1 activity when compared with control selenium-supplemented S126 cells (Table I). Although the ^{75}Se-labeled p27^{wt} was completely lost in selenium-deficient cells, the cellular content of M4 was unaffected by changes in selenium content. Estimates of the p27^{wt} and M4 content in selenium-supplemented S126 cells (Table I) showed that there is an ~10-fold molar excess of M4 over the native p27^{wt}, and based on the data in Fig. 3 and in Table I this appears to be sufficient to complex most, if not all, of the native p27^{wt} present in the S126 cell (Table I).

TABLE I
Summary of the D1 activity, M4, and p27^{wt} content in S126 cells

M4 content was determined by competitive binding assay as described under "Experimental Procedures" using ^{125}I-labeled peptide as the tracer. Wild type p27 content was determined by measuring the quantity of ^{75}Se-labeled native p27 in S126 cells after radiolabeling to equilibrium and SDS-PAGE analysis. 1 unit of D1 activity = 1 pmol I$^-$ released/min. ND, not detected (<0.001 pmol/mg protein). Data are reported as means ± S.E., n = 3.

	Growth conditions	
	No ^{75}Se	40 nM ^{75}Se
D1 activity (units/mg protein)	1.5 ± 0.2	19.1 ± 3.1
M4 (pmol/mg protein)	1.7 ± 0.2	1.6 ± 0.30
p27^{wt} (pmol/mg protein)	ND	0.17 ± 0.03
Molar ratio M4/p27^{wt}	>1000	9.4

Physiochemical Properties of the Hybrid D1 Composed of p27^{wt}-M4 Partners in S126 Cells—To determine whether the catalytically active hybrid D1 composed of p27^{wt}-M4 partners was a dimer or a higher order aggregate, detergent extracts of ^{75}Se-labeled S126 cells were separated by isopycnic density gradient centrifugation (28), and the sedimentation properties of the ^{75}Se-labeled p27^{wt}-M4 partners were determined by immune precipitation. The distribution of ^{75}Se-labeled p27^{wt}-M4 complexes peaked between the marker proteins carbonic anhydrase and BSA as shown in Fig. 5. Assuming a frictional ratio (f/f_0) of 0.85 equal to that determined for BrAcT$_4$-labeled p27 (28), the sedimentation coefficient ($s_{20,w}$) for the ^{75}Se-labeled hybrid D1 (p27^{wt}-M4 complex) is ~3.5, yielding a calculated mass of 54 kDa in close agreement with previous estimates of the native D1 (28). These data confirm that the catalytically active hybrid D1 in S126 cells is a dimer composed of one p27^{wt} and one M4 subunit.

The Role of the Membrane Anchor in D1 Holoenzyme Assembly—Since the D1 holoenzyme is a dimer of two membrane-spanning p27 subunits and assembly of the enzyme is a post-translational event, we examined the role of the membrane anchor in D1 holoenzyme assembly. Earlier work suggested that the N terminus of p27 was required for either proper post-translational processing or that specific residues located in this region were necessary for catalysis. Two basic residues in the N terminus of p27 appear to be required for proper folding of the p27 (10). To explore the role of the membrane anchor of p27 in D1 assembly, we prepared N-terminal deletion mutants of M4 in which the "external" 12 amino acids, including two basic residues at position 11 and 12, and 7 residues in the membrane-spanning region were removed (M4-19), and/or the entire membrane anchor was deleted (M4-42). Constitutive overexpression of these truncation mutants in LLC-PK1 cells was done as described for the parent M4 and yielded two new cell lines, M4-19 and M4-42.

Shown in Fig. 6, are the consequences of expression of M4-19 and M4-42 on D1 activity. As observed with the parent M4, overexpression of either truncation mutation decreased D1 activity by ~50%, and 90–95% of the D1 activity present in the M4-19 and M4-42 cells was immunoprecipitated by the anti-rat p27 antibody. These data indicate that a catalytically active D1 holoenzyme can be formed from dimers of the native p27^{wt} and a truncated p27 that lack the entire membrane anchor. From these data it appears that assembly of the D1 holoenzyme does not require both p27 subunits to be membrane-associated.

Catalytic Consequences of Hybrid D1 Holoenzyme Composed of p27^{wt} and Inactive Subunits—Since the D1 activity in the S126 cell was derived from a holoenzyme composed of p27^{wt}-M4
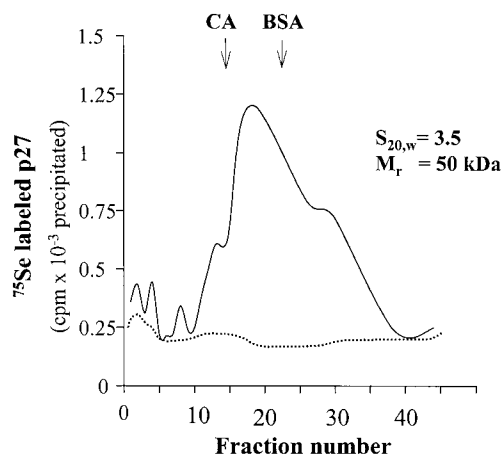
FIG. 5. Migration of D1 holoenzyme composed of p27^{wt}-M4 in 5–20% linear sucrose gradients in H$_2$O. D1 holoenzyme was labeled with ^{75}Se and solubilized from S126 cells (*solid line*) and control LLC-PK1 cells (*dotted line*) with 5 mM tDOC as described under "Experimental Procedures." One mg of solubilized protein was sedimented on individual gradients as described previously (22, 28). Carbonic anhydrase (*CA*) and BSA were added internal standard proteins and identified on stained SDS-PAGE gels on individual fractions. ^{75}Se-labeled protein associated with M4 was immune precipitated with anti-rat p27 antisera as described under "Experimental Procedures" and counted in a well-type γ-counter. Data are representative of 3 separate gradients.
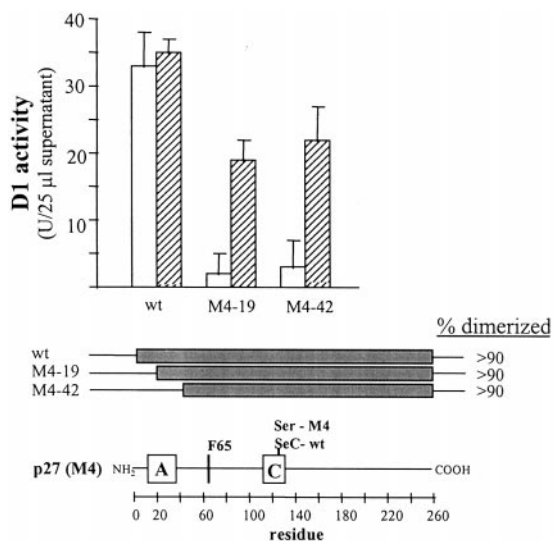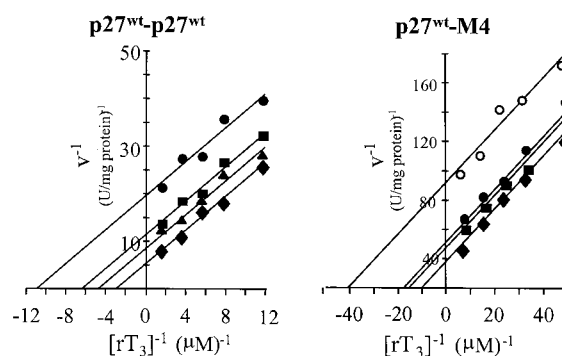

FIG. 6. Effects of the N-terminal membrane anchor of p27 on assembly of catalytically active D1 holoenzyme. N-terminal truncation mutants (M4-19 and M4-42) were prepared as described under "Experimental Procedures" and transfected into LLC-PK1 cells, and stable transfectants were selected with 800 μg/ml G418. Cell membranes were prepared and immunoprecipitated with anti-rat p27 antisera (1:100 final dilution) as described in the legend to Fig. 1*B*. Data reported as means ± S.E. $n = 3$ independent membrane preparations. Also shown are the putative p27 domains remaining in each truncation mutant. *A*, membrane anchor; *C*, catalytic domain.
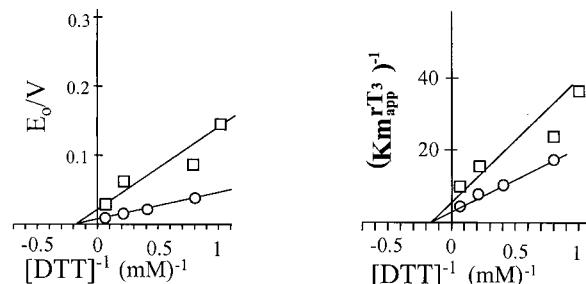

FIG. 7. Initial velocity reaction kinetics for D1 activity in control LLC-PK1 cells carrying the empty pcDNA3 vector (D1 wild type) and in S126 cells (M4). Steady-state reaction kinetics were done as described previously (24, 29). The hybrid D1 holoenzyme was obtained from the S126 cells detailed in Table I, and the enzyme concentration was assumed to be equal to that of the native p27 (~0.2 pmol/mg cell protein). ○, 1.0; ●, 1.67; ■, 2.5; ▲, 5; ◆, 20 mM dithiothreitol (*DTT*). Intercept replots: ○, wild type D1; □, S126 D1. Data are representative of 3 separate studies. All lines were drawn by least squares linear regression analysis.

TABLE II
Limiting kinetic constants for wild type D1 and the hybrid D1 in S126 cells

Molar activity = mol product · min^{-1} · mol D1 holoenzyme^{-1}. Data reported as means ± S.E., $n = 3$ for separate determinations. DTT, dithiothreitol.

D1 dimer composition	Limiting K_m		Molar activity
	rT$_3$	DTT	
	μM	mM	
p27^{wt}-p27^{wt}	0.5	7.5	1780 ± 100
p27^{wt}-M4	0.2	7.5	447 ± 40

subunits, and M4-M4 dimers are catalytically inert, we used the hybrid D1 activity in S126 cells to examine the influence of each subunit on the catalytic reaction. Hybrid D1 activity was provided by S126 cell lysates, and two-substrate reaction kinetics were done as detailed previously (24, 29). As shown in Fig. 7, both wild type D1 activity in LLC-PK1 cells and the hybrid D1 activity derived from p27^{wt}-M4 dimers in S126 cells showed the expected ping-pong reaction kinetics. Secondary replots of slopes and intercepts *versus* the reciprocal of the thiol cofactor concentration yielded the limiting kinetic constants of the respective D1 holoenzyme (Table II). Although the limiting K_m values for the thiol cofactor and iodothyronine were either

unchanged or marginally affected when one of the p27 subunits was catalytically inert, there was a marked 75% reduction in the maximal forward velocity of the deiodination reaction of the hybrid D1 when compared with that of the wild type D1.

Subcellular Distribution of M4^{GFP}-M4^{GFP} Dimers and p27^{wt}-M4^{GFP} Dimers in S126 Cells—Finally, we exploited the fact that the C terminus of p27 is degenerate, to generate a fluorescent p27-green fluorescent protein reporter molecule (GFP) fusion protein (M4^{GFP}) that allows the D1 holoenzyme to be followed in the living cell. GFP was appended in-frame to the C terminus of M4, and constitutive expression of the M4^{GFP} fusion protein in LLC-PK1 cells led to the appearance of abundant membrane-bound fluorescence (Fig. 8). D1 activity in the M4^{GFP}-expressing cells showed a marked decrease (45 units/mg protein in control LLC-PK1 cells *versus* 18 units/mg protein in M4^{GFP}-expressing cells) similar to that observed when M4 alone was introduced into the LLC-PK1 cell (see Fig.
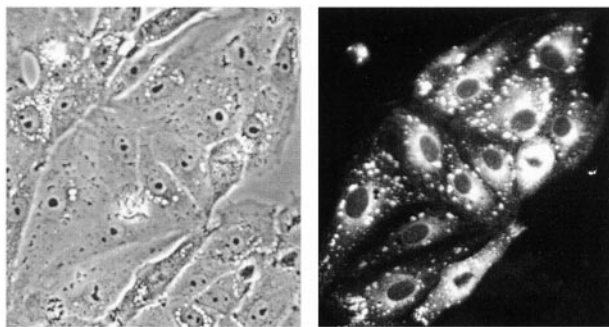
FIG. 8. **Representative photomicrographs of S126 cells constitutively expressing M4^{GFP}.** Phase contrast images of the M4^{GFP}-expressing (*left panel*) and companion fluorescence images of the same field (*right panel*). *Sizing bar = 20 μm.*

3). These findings show that addition of the GFP reporter to the C terminus of M4 did not impair the ability of M4 to form hybrid D1 dimers with the native p27^{wt} subunit. To ensure that the D1 activity present in the M4^{GFP}-expressing cells was derived from a hybrid D1 holoenzyme composed of native p27^{wt} and M4^{GFP} subunits, anti-GFP antibodies were used in a pulldown assay. As expected, anti-GFP IgG did not precipitate the D1 activity in control LLC-PK1 cell extracts but specifically immunoprecipitated >95% of the D1 activity in M4^{GFP}-expressing cells (data not shown). These findings show that overexpression of the inert D1 subunit, M4^{GFP}, results in the formation of a catalytically active D1 holoenzyme composed of a p27^{wt} and M4^{GFP} subunits and that the appended GFP reporter had little, if any, influence on the deiodination reaction of the complex.

Shown in Fig. 8 are representative photomicrographs of the distribution of the M4^{GFP}-derived D1 holoenzyme in LLC-PK1 cells constitutively expressing this fusion protein (M4^{GFP} cells). Abundant punctate florescent signals were found between the boundaries of adjacent cells and along the cell periphery of individual cells. Infrequently, a more diffuse fluorescent signal is observed in the perinuclear space. These data are consistent with earlier studies showing that the BrAcT$_4$-labeled native p27^{wt} was sorted to the basolateral membranes in the oriented LLC-PK1 cell (23, 27, 30) and indicate that the M4^{GFP} fusion protein, whether as a homodimer or a mixed wild type p27:M4^{GFP}, is also directed to the basolateral plasma membrane.

DISCUSSION

Thyroid hormone deiodination catalyzed by D1 generates most of the bioactive T$_3$ found in the circulation and thereby plays a key role in the molecular mechanism of thyroid hormone action. Although the cloning of p27 yielded a catalytically active D1 after transient transfection (5), the subunit composition of the active enzyme, the role of individual p27 polypeptides in the catalytic reaction, and the physiochemical properties of the cloned enzyme have not been determined. In this report, we describe the subunit composition of catalytically active D1 holoenzyme, examine the role of each subunit in the deiodination reaction, and show that the D1 dimer is sorted to the basolateral plasma membrane of renal epithelial cells.

Prior to the cloning of p27, affinity labeling studies done with alkylating derivatives of thyroxine were used to identify the D1 polypeptide(s). In both liver and kidney membrane preparations, a 27-kDa BrAcT$_4$-labeled protein was identified, and this protein showed all of the properties of the substrate binding component of D1 as judged by rate inactivation studies (23) and inhibitor competition studies (19, 20). Subsequent work showed that the p27 polypeptide and the active D1 enzyme could not be separated by gel filtration and/or isopycnic density gradient

centrifugation and that the molecular mass of the BrAcT$_4$-labeled D1 was 54 kDa with an $s_{20,w}$ of 3.7 S (28), values similar to those determined earlier for a detergent-soluble D1 that required reactivation by lipid reconstitution (22). In contrast, detergent extracts of liver D1 that contained a catalytically active proteolipid complex showed a family of active enzyme(s) with much larger molecular weights after gel filtration (31, 32). Thus, the constitution of the membrane-bound, functional D1 appeared to differ according to the detergent used and the tissue source.

The finding that a catalytically active D1 enzyme assembles from an exogenous, inert p27 and a native p27 and that the hybrid enzyme had the same physiochemical properties as the native D1 directly confirms that D1 is a homodimer of p27 subunits. This is consistent with the earlier work (22, 23) that followed soluble D1 activity in crude membrane extracts. In addition, this observation shows that native and mutant p27 subunits can combine to constitute a hybrid enzyme and reveals that D1 assembly is a post-translational event that presumably depends upon the local concentration of p27 in the membrane. Since overexpression of an exogenous p27 mutant drives the native p27 subunit into hybrid D1 molecules, it appears that both the assembly and the composition of the D1 holoenzyme can be predetermined by experimental manipulation.

Assembly of a functional D1 holoenzyme not only requires sufficient numbers of p27 subunits but also the correct positioning of yet to be identified dimerization domain(s). Importantly, the orientation of the native p27^{wt} subunits in the D1 holoenzyme is constrained to a head-to-head, tail-to-tail orientation by the polarity of the membrane-bound p27 subunits and the sidedness of the catalytic activity (23, 30). This limiting constraint imposed by the membrane-bound nature of p27 led Larsen and co-workers (10) to conclude that residues within the p27 membrane anchor directed either the proper folding of the p27 or participated in catalysis. Their conclusions were based, in part, on the failure of several p27 mutants to generate D1 activity after transient transfection when the membrane anchor of p27 was swapped with the endoplasmic reticulum-derived membrane anchor(s) from the bovine 21-hydroxylase P450 enzyme (10). The results detailed in Fig. 7 clearly show that truncated p27 subunits lacking the membrane anchor will bind to the native p27 and produce a functional D1 holoenzyme in which only one p27 subunit is anchored to the membrane. These findings indicate that the assembly of the D1 holoenzyme is independent of the membrane anchor. Thus, the failure of the membrane anchor swapped p27s to assemble into a functional enzyme (10) is likely due to the low abundance of the exogenous p27 selenoprotein translation products after transient transfection and/or to directional miscues given by the endoplasmic reticulum resident P450-derived membrane anchor. Similar caveats apply to the failure of the p27 mutants in which the membrane anchor derived from the deiodinase family member, type III iodothyronine 5'-deiodinase, was substituted for the native membrane-spanning region to generate catalytically active enzyme (10). Since loss of the membrane anchor from one p27 subunit yields a hybrid D1 with activity levels similar to that found when both enzyme subunits are membrane-bound, it is likely that a catalytically active, "soluble" D1 holoenzyme would assemble if sufficient quantities of truncated p27 selenoprotein subunits could be produced. Unfortunately, the limiting quantity of SeC in mammalian cells is likely to interfere with the synthesis of sufficient quantities of soluble p27 selenoprotein necessary to drive assembly of a soluble D1 holoenzyme.

With the composition of the catalytically active D1 holoen-

zyme established, it is now possible to revisit the role of individual amino acids in the catalytic reaction and in enzyme assembly. For example, whereas site-directed mutagenesis was used to identify both the SeC and His as essential enzyme residues, these data did little to extend earlier work using more traditional approaches of chemical modification (16, 18, 33–37). In fact, among the histidine residues present in p27, D1 activity was completely lost by mutations of His-158 barring further analysis of this essential residue (13). Examination of the primary amino acid sequence of p27 reveals that this residue is located in the middle of an ~15-residue long stretch found in all deiodinase family members from frog to man. With the ability to predetermine the composition of D1 holoenzyme, the influence of His-158 and His-174 on catalysis and on enzyme assembly can now be directly evaluated.

The ability to drive a native, catalytically active p27 subunit into partnership with an inert p27 mutant allowed us to evaluate the catalytic reaction in a D1 holoenzyme in which only one partner is functional. By using steady-state reaction kinetics, we found that the hybrid D1 holoenzyme had little, if any, change in substrate affinities but showed a 75% decrease in the molar activity compared with wild type D1 dimer. Whether this decrease in activity reflects an interaction between the inert subunit and the native p27 that lowers the intrinsic catalytic potential of the native p27 or indicates that each p27 subunit in the D1 holoenzyme can serve as a catalytic center remains to be established.

Based on the degeneracy of the C terminus of p27, we generated an inert p27^{GFP} fusion protein that could be followed in the living cell. Addition of this relatively large epitope did not affect the ability of the fusion protein (M4GFP) to partner with the wild type p27 in LLC-PK1 cells, and the fluorescent D1 holoenzyme showed the same catalytic properties as that for D1 holoenzyme composed of M4 and p27^{wt} subunits. Assuming the same stoichiometry of p27^{GFP} fusion protein and p27^{wt} as described in Table I, then ~10% of the florescent D1 dimers were composed of an inert and active subunit, whereas 90% of the dimers formed were composed of two fluorescent and inert p27s. Analysis of the subcellular distribution of fluorescent D1 dimers revealed that the D1 dimers were sorted to the basolateral membranes of the oriented renal epithelial cell (23, 30).

In conclusion, the data show that catalytically active D1 is a homodimer of p27 subunits and that hybrid enzyme with only one active subunit can catalyze deiodination by a ping-pong reaction mechanism. Although the membrane anchor located in the N terminus of p27 constrains the assembly of the D1 subunits into a head-to-head and tail-to-tail orientation, p27 dimerization does not require the membrane anchor, and enzyme assembly is a post-translational event that appears to be driven by the local concentrations of enzyme subunits. Once assembled the D1 holoenzyme is sorted to the plasma membrane in both kidney and liver cells, where it can serve as an enzymic barrier to the entry of the prohormone T_4 and the source of bioactive T_3 for the cell.

REFERENCES

1. Larsen, P. R., and Berry, M. J. (1994) *Thyroid* **4,** 357–362
2. Leonard, J. L., and Visser, T. J. (1986) in *Thyroid Hormone Metabolism* (Hennemann, G., ed) pp. 189–229, Marcel Dekker, Inc., New York
3. Köhrle, J., Brabant, G., and Hesch, R. D. (1987) *Horm. Res. (Basel)* **26,** 58–78
4. Visser, T. J. (1996) *Acta Med. Austriaca* **23,** 10–16
5. Berry, M. J., Banu, L., and Larsen, P. R. (1991) *Nature* **349,** 438–440
6. Behne, D., Kyriakopoulos, A., Meinhold, H., and Köhrle, J. (1990) *Biochem. Biophys. Res. Commun.* **173,** 1143–1149
7. Berry, M. J., Kieffer, J. D., Harney, J. W., and Larsen, P. R. (1991) *J. Biol. Chem.* **266,** 14155–14158
8. Sanders, J. P., Van der Geyten, S., Kaptein, E., Darras, V. M., Kühn, E. R., Leonard, J. L., and Visser, T. J. (1997) *Endocrinology* **138,** 5153–5160
9. Toyoda, N., Harney, J. W., Berry, M. J., and Larsen, P. R. (1994) *J. Biol. Chem.* **269,** 20329–20334
10. Toyoda, N., Berry, M. J., Harney, J. W., and Larsen, P. R. (1995) *J. Biol. Chem.* **270,** 12310–12318
11. Toyoda, N., Kaptein, E., Berry, M. J., Harney, J. W., Larsen, P. R., and Visser, T. J. (1997) *Endocrinology* **138,** 213–219
12. Berry, M. J., Maia, A. L., Kieffer, J. D., Harney, J. W., and Larsen, P. R. (1992) *Endocrinology* **131,** 1848–1852
13. Berry, M. J. (1992) *J. Biol. Chem.* **267,** 18055–18059
14. Croteau, W., Bodwell, J. E., Richardson, J. M., and St Germain, D. L. (1998) *J. Biol. Chem.* **273,** 25230–25236
15. Sun, B. C., Harney, J. W., Berry, M. J., and Larsen, P. R. (1997) *Endocrinology* **138,** 5452–5458
16. Mol, J. A., Docter, R., Hennemann, G., and Visser, T. J. (1984) *Biochem. Biophys. Res. Commun.* **120,** 28–36
17. Goswami, A., and Rosenberg, I. N. (1990) *Biochem. Biophys. Res. Commun.* **173,** 6–12
18. Mol, J. A., Docter, R., Kaptein, E., Jansen, G., Hennemann, G., and Visser, T. J. (1984) *Biochem. Biophys. Res. Commun.* **124,** 475–483
19. Köhrle, J., Rasmussen, U. B., Ekenbarger, D. M., Alex, S., Rokos, H., Hesch, R. D., and Leonard, J. L. (1990) *J. Biol. Chem.* **265,** 6155–6163
20. Köhrle, J., Rasmussen, U. B., Rokos, H., Leonard, J. L., and Hesch, R. D. (1990) *J. Biol. Chem.* **265,** 6146–6154
21. Safran, M., Köhrle, J., Braverman, L. E., and Leonard, J. L. (1990) *Endocrinology* **126,** 826–831
22. Leonard, J. L., and Rosenberg, I. N. (1981) *Biochim. Biophys. Acta* **659,** 205–218
23. Leonard, J. L., Ekenbarger, D. M., Frank, S. J., Farwell, A. P., and Koehrle, J. (1991) *J. Biol. Chem.* **266,** 11262–11269
24. Leonard, J. L., and Rosenberg, I. N. (1980) *Endocrinology* **107,** 1376–1383
25. Sanger, F., Nicklen, S., and Coulson, A. R. (1977) *Proc. Natl. Acad. Sci. U. S. A.* **74,** 5463–5467
26. Larsen, P. R. (1997) *Biochem. Soc. Trans.* **25,** 588–592
27. Leonard, J. L., and Rosenberg, I. N. (1978) *Endocrinology* **103,** 274–280
28. Safran, M., and Leonard, J. L. (1991) *J. Biol. Chem.* **266,** 3233–3238
29. Leonard, J. L., and Rosenberg, I. N. (1978) *Endocrinology* **103,** 2137–2144
30. Prabakaran, D., Ahima, R. S., Harney, J. W., Berry, M. J., Larsen, P. R., and Arvan, P. (1999) *J. Cell Sci.* **112,** 1247–1256
31. Fekkes, D., van Overmeeren, E., Hennemann, G., and Visser, T. J. (1980) *Biochim. Biophys. Acta* **613,** 41–51
32. Fekkes, D., Hennemann, G., and Visser, T. J. (1983) *Biochim. Biophys. Acta* **742,** 324–333
33. Visser, T. J. (1980) *Biochim. Biophys. Acta* **611,** 371–378
34. Visser, T. J., Kaptein, E., and Aboul-Enein, H. Y. (1992) *Biochem. Biophys. Res. Commun.* **189,** 1362–1367
35. Schoenmakers, C. H., Pigmans, I. G., and Visser, T. J. (1992) *Biochim. Biophys. Acta* **1121,** 160–166
36. Leonard, J. L., and Visser, T. J. (1984) *Biochim. Biophys. Acta* **787,** 122–130
37. Fekkes, D., Hennemann, G., and Visser, T. J. (1982) *FEBS Lett.* **137,** 40–44

Jack L. Leonard, Theo J. Visser and Deborah M. Leonard

Access the most updated version of this article at doi: 10.1074/jbc.M006973200

Find articles, minireviews, Reflections and Classics on similar topics on the JBC Affinity Sites.

Alerts:

- When this article is cited
- When a correction for this article is posted

Click here to choose from all of JBC's e-mail alerts

This article cites 36 references, 12 of which can be accessed free at
http://www.jbc.org/content/276/4/2600.full.html#ref-list-1